RRW Framework by Using Enhanced Pixel Wise masking and K-Means Clustering

N. Krishna Chaitanya[1], Vijaya Kumar Nasina[2]

[1]*Associate Professor, ECE Department, PBR VITS, KAVALI, NELLORE (DT.), INDIA*
[2]*Student M.Tech(DSCE), ECE Department, PBR VITS, KAVALI, NELLORE (DT.), INDIA*

Abstract: *This paper presents Robust reversible watermarking methods are popular in multimedia for protecting copyright, while preserving intactness of host images and providing robustness against unintentional attacks. However, conventional RRW methods are not readily applicable in practice. That is mainly because they fail to offer satisfactory reversibility on large-scale image datasets. They have limited robustness in extracting watermarks from the watermarked images destroyed by different unintentional attack. Some of them suffer from extremely poor invisibility for watermarked images. Therefore, it is necessary to have a framework to address these three problems, and further improve its performance. So a novel pragmatic framework is proposed that is wavelet-domain statistical quantity histogram shifting and clustering (WSQH-SC). Compared with conventional methods, WSQH-SC ingeniously constructs new watermark embedding and extraction procedures by histogram shifting and clustering, which are important for improving robustness and reducing run-time complexity. Additionally, WSQH-SC includes the property-inspired pixel adjustment to effectively handle overflow and underflow of pixels. This results in satisfactory reversibility and invisibility. Furthermore, to increase its practical applicability, WSQH-SC designs an enhanced pixel-wise masking to balance robustness and invisibility. So it perform extensive experiments over natural, medical, and synthetic aperture radar images to show the effectiveness of WSQH-SC by comparing with the histogram rotation-based and histogram distribution constrained methods.*

Key words: *Integer wavelet transform, k-means clustering, masking, robust reversible watermarking (RRW).*

I.   Introduction

REVERSIBLE WATERMARKING (RW) methods [1] are used to embed watermarks [2], e.g., secret information [3], into digital media while preserving high intactness and good fidelity of host media. It plays an important role in protecting copyright and content of digital media for sensitive applications, e.g., medical and military images. Although researchers proposed some RW methods for various media, e.g., images [4], [5], audios [6], videos [7], and 3-Dmeshes [8], they assume the transmission channel is lossless. The robust RW (RRW) is thus a challenging task. For RRW, the essential objective is to accomplish watermark embedding and extraction in both lossless and lossy environment. As a result, RRW is required to not only recover host images and watermarks without distortion for the lossless channel, but also resist unintentional attacks and extract as many watermarks as possible for the noised channel [9].

II.   Existing Methods

Recently, a dozen of RRW methods for digital images have been proposed [10]–[13], which can be classified into two groups [9]: histogram rotation (HR)-based methods and histogram distribution constrained (HDC) methods. The HR-based methods [10], [11] accomplish robust lossless embedding by slightly rotating the centroid vectors of two random zones in the non-overlapping blocks. Due to the close correlation of neighboring pixels, these methods were reported to be robust against JPEG compression. However, they are sensitive to "salt-and-pepper" noise, which leads to poor visual quality of watermarked images, and impedes lossless recovery of host images and watermarks. To solve this problem, the HDC methods have been developed in spatial and wavelet-domains [12], [13], which divide image blocks into different types and embed the modulated watermarks for each type based on histogram distribution. Unfortunately, these methods suffer from unstable reversibility and robustness according to [9]. In summary, the above analysis shows that both kinds of RRW methods are not readily applicable in practice.

III. Proposed Framework

In this section, we introduce a new RRW framework, i.e., WSQH-SC, which accomplishes the robust lossless embedding task by incorporating the merits of SQH shifting, k-means clustering and EPWM. WSQH-SC comprises two processes: watermark embedding and extraction. In view of their similarity, Fig. 1 only shows the diagram of the embedding process in which the three modules are termed: 1) PIPA; 2) SQH construction; and 3) EPWM-based embedding, and they are detailed in the following three subsections. To be specific,

WSQH-SC first investigates the wavelet sub-band properties in depth and exploits PIPA to preprocess the host image, which is of great importance to avoid both overflow and underflow of pixels during the embedding process. Afterward, the host image is decomposed by the 5/3 integer wavelet transform (IWT) [30] and the blocks of interest in the sub-band C_0^{HL} are selected to generate the SQH with the help of the threshold constraint. Finally, watermarks can be embedded into the selected blocks by histogram shifting, wherein EPWM is designed to adaptively control watermark strength. After the IWT reconstruction, the watermarked image is obtained.
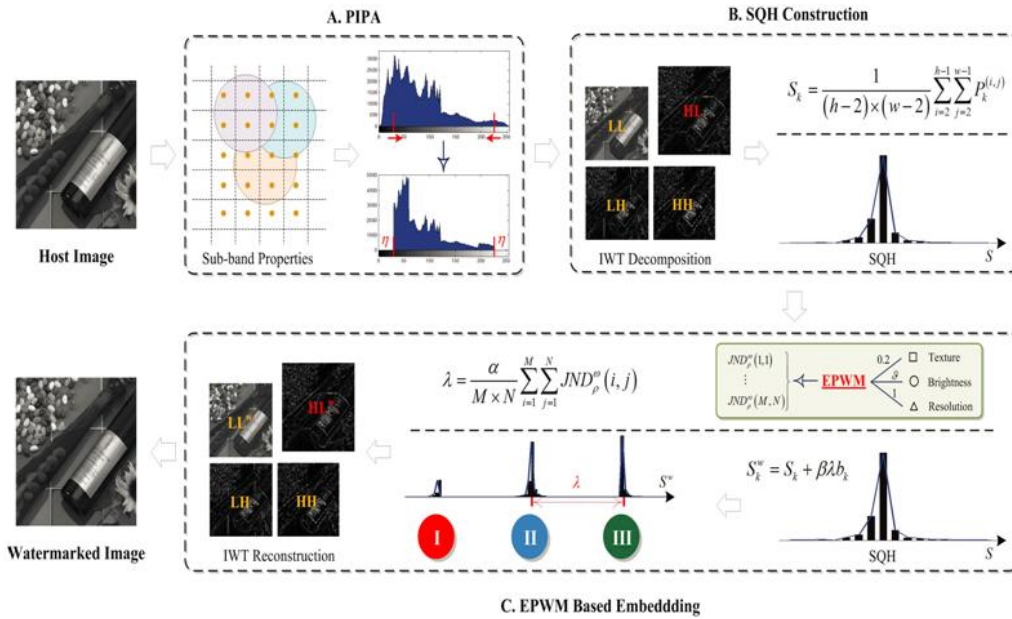

Fig. 1. Embedding process of the proposed wavelet-domain SQH shifting and clustering framework.
(a)   PIPA.   (b)   SQH   construction.   (c)   EPWM   based   embedding

A. PIPA:

Firstly, PIPA deeply exploits the intrinsic relationship between wavelet coefficient and pixel changes. Secondly, by taking the scale and region of wavelet coefficient changes into consideration, PIPA determines the adjustment scale and employs the pixel adjustment strategy to preprocess the host images.

Multiple Sub-Bands and Multiple Wavelet Coefficients:

Considering an arbitrary block with the top left corner at (p, q) in C_0^W , $1 \le p < M$, $1 \le q < N$, we investigate the changes of wavelet coefficients and pixels in two special cases, Here, $v_f =$ $[0,0,1,0,1,0\ldots1,0,0]_{2xh-1}$, $v_g = [1,2,\ldots2,1]_{2xw-3}$ and the affected region of pixels is denoted by the location of its top left corner. To further illustrate such effects, Fig. 2 shows an example in which the block size is 3 × 3, and the wavelet coefficients of two neighboring blocks in C_0^{LL} and C_0^{HL} are changed simultaneously.
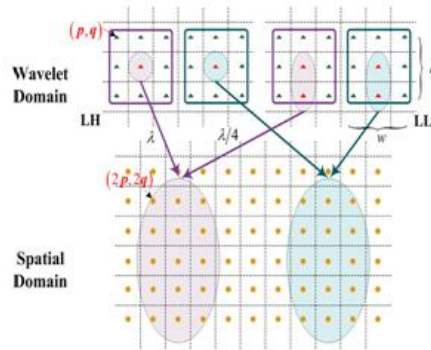

Fig. 2. Example of the effects of changing wavelet coefficients on pixels based on multiple sub-bands and multiple wavelet coefficients.

With Fig. 2, we can deduce that: 1) the affected pixel regions are nonoverlapped when the wavelet coefficients of neighboring blocks are changed at the same time and 2) the pixel changes are monodirectional and the maximum change scale equals λ. In this case, we can easily determine the adjustment scale and use the pixel adjustment strategy to preprocess host images. In particular, given a t-bit host image I with the size of 2M ×2N, the pixel adjustment is performed by

$$I^!(i,j) = \begin{cases} I(i,j) - \eta, & if.I(i,j) > 2^t - \eta \\ I(i,j) + \eta, & if.I(i,j) < \eta \end{cases} \quad (1)$$

where I (i, j) is the grayscale value of the pixel at (i, j) in the image I , I(i, j) is the adjusted one (1 ≤ i ≤ 2M, 1 ≤ j ≤ 2N), and η > λ is the adjustment scale. Thereafter, the preprocessed host image can be reliably used for watermark embedding in the next subsections. Because the pixels are changed into a reliable range before embedding, i.e.[η, 2t − 1 − η], PIPA can successfully avoid both overflow and underflow of pixels [15]. It is also worth emphasizing that the proposed WSQH-SC is nonblind to some extent because the locations of the changed pixels need to be saved as a part of side information and transmitted to the receiver side in order to recover the original grayscale values of pixels.

B. SQH Construction
In this subsection, we consider the SQH construction task with a threshold constraint. Inspired by characteristics of the wavelet coefficients [13], we focus on the mean of wavelet coefficients (MWC) histogram by taking the following two properties into account: 1) it is designed in high-pass sub-bands of wavelet decomposition, to which HVS is less sensitive, leading to high invisibility of watermarked images and 2) it has almost a zero-mean and Laplacian-like distribution based on the experimental study of wavelet high-pass sub-bands from 300 test images illustrated in Section V, which is stable for different images. In particular, an MWC histogram is generated based on the following procedure. Considering a given host image I , we first decompose I using 5/3 IWT to obtain the sub-band C_0^{HL} , and then divide C_0^{HL} into n nonoverlapping blocks.

Let S = [S_1, . . . , S_k, . . . , Sn] be the MWCs in the sub-band, then the MWC of the kth kth block, S_k is defined as

$$S_k = \frac{1}{(h-2)X(w-2)} \sum_{i=2}^{h-1} \sum_{j=2}^{w-1} p_k^{(i,j)} \quad (2)$$

where $P_k^{(i,j)}$ represents the wavelet coefficient at (i, j) in the kth block. To construct the MWC histogram, our concern is the possibility of utilizing the blocks of interest in a sub-band,
which will be helpful for simplifying the embedding process.In view of the histogram distribution of MWC, only the peak and its neighbors in the histogram are mostly useful for the
embedding task. Therefore, a threshold constraint is applied to the blocks to retain those of interest, each of which satisfies the following condition:

d (x, S_k) ≤ δ, 1 ≤ k ≤ n   (3)

where d (·) computes the Euclidean distance of two elements, x ∈ {xl , xr } represents the aforementioned two peak points, and δ is a predefined constant for threshold control. When

δ ≥ max {d (X_1 , min (S)) , d (X_r , max (S))}, all of the blocks will be retained for embedding, which is a special case of this constraint. Moreover, with the help of the threshold constraint, the capacity can be controlled flexibly.

C. EPWM-Based Embedding :
It has been well acknowledged that a balance between invisibility and robustness is important for robust watermarking methods. Although many efforts have been made to design lossless embedding models, little progress has been made in this trade-off. Therefore, we develop EPWM to tackle this problem by utilizing the JND thresholds of wavelet coefficients to optimize watermark strength. In view of the disadvantages of PWM discussed in Section II, EPWM focuses on improving the local sensitivity of images to noise by mainly estimating brightness and texture sensitivities in a more precise way. Motivated by the benefits of luminance masking [34], we first redefine the brightness sensitivity in (5) by calculating the luminance masking of the low-pass sub-band at resolution level ρ, denoted as

$$\psi(\rho,i,j) = \max\{ f_g^\rho (l_v^\rho(i,j)), f_s^\rho (l_b^\rho(i,j), l_m^\rho(i,j))\} \quad (4)$$

$$I^1(i,j) = \begin{cases} (3/128) \cdot (l_b^\rho(\cdot) - 127) + 3, l_b^\rho(\cdot) > 127 \\ 17 \cdot (1 - \sqrt{l_b^\rho(\cdot)/127}) + 3, l_b^\rho(\cdot) \le 127 \end{cases} \qquad (5)$$

And

$$f_s^p(l_b^\rho(\cdot), l_m^\rho(\cdot)) = l_m^\rho(\cdot) d_1(l_b^\rho(\cdot)) + d_2 l_b^\rho(\cdot)) \text{ -(6)}$$

represent the visibility threshold and spatial masking functions, respectively, in which d1 (·) and d2 (·) are the background luminance dependent functions, and lρ b (·) and lρm (·) mean
the average background luminance and maximum weighted average of luminance differences. Then, the texture sensitivity is evaluated based on [35] by

$$\prod(\rho, i, j) = \sum_{k=0}^{3-\rho} \frac{1}{16^k} \sum_{w \in [LH, HL, HH]} \sum_{x=0}^{1} \sum_{y=0}^{1} [C_{k+\rho}^w (y + \frac{i}{2^k}, x + \frac{j}{2^k})]^2 \times \frac{1}{\gamma_\rho^3} \gamma_\rho^3 \text{ (I,j)} \qquad (7)$$
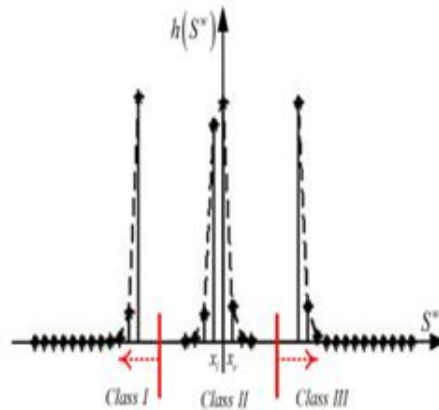

Fig. 3: Example of WMC histogram in a watermarked image.

Algorithm1: Proposed Classification Process

Input: The MWCs $S^w = [S_1^w, \ldots, S_m^w]$, and number of clusters μ.

Output: The set of clusters g =[$g_1, \ldots, g_\mu$]

1. Inittialize the clusters $f_1^{(1)}, \ldots, f_\mu^{(1)}$, iteration time ε;
2. Do
3. For k=1 to m do

4 Assign the kth S_w^k to one of the clusters according to the distance between it and cluster centers.

$S_w^k \in g_j$, if d($S_w^k, f_j^{(\varepsilon)}) \le d(S_w^k, f_l^{(\varepsilon)})$ *for all* $l = 1, 2, \ldots, \mu$

5 **End for**

6 Update the cluster centers with $f_j^{(\varepsilon+1)} = (1/|g_j^{(\varepsilon)}|) \cdot \sum_{S_w^k \in g_j^{(\varepsilon)}} S_w^k$

7 While arg $\min \sum_{j=1}^{\mu} \sum_{S_w^k \in gj} || S_w^k - f_j^{(\varepsilon+1)} ||^2$

where □ 3 ρ is the mean of the approximation sub-image □3 ρ . Because both (13) and (16) take the difference between resolution levels into account, we can replace (6) with

$$\theta(w) = \begin{cases} \sqrt{2}, & \text{if } w = HH \\ 1, & \text{Otherwise} \end{cases} \qquad (8)$$

Finally, the new JND threshold can be obtained by

$$JND_p^w = \theta(w) \psi(\rho, i, j)^9 \pi(\rho, i, j)^{0.2} \qquad (9)$$

in which $0 < \square \leq 1$ is a tuning parameter corresponding to the weight of brightness sensitivity. In view of space limitation, refer to [15] and [16] for the definitions of d1 (·), d2 (·), lρ b (·), lρm (·), and $\square 3\ \rho$. With (8), we use the obtained JND thresholds to control watermark strength during the embedding process. To be specific, given the MWC of the kth block of interest, i.e., Sk, $1 \leq k \leq m$, the watermark embedding is given by

$$S_w^k = S_k + \beta\lambda b_k \quad (10)$$

Here S_w^k is the obtained MWC after the kth watermark bit $b_k \in \{0, 1\}$ is embedded, β is a factor defined as

$$\beta = (S_k\text{-}S^*)/\text{abs}(S_k\text{-}S^*) \quad (11)$$

$$S^* = \arg\min d(S_k,\text{x})$$
$$\text{x}\in x_l, x_r)$$

$$\lambda = \frac{\alpha}{M\ x\ N} \sum_{i=1}^{M} \sum_{j=1}^{N} JND_\rho^w\ (i,j) \quad (12)$$

represents the watermark strength, where α is a global parameter and M × N is the sub-band size. Because the novel embedding model shown in (10) expands the additive spread

spectrum [36] to a reversible embedding model, we term it a generalized additive spread spectrum. By applying (10) to the blocks of interest in the sub-band, watermarks can be

embedded into the wavelet coefficients. Thereafter, the IWT reconstruction is performed to obtain the watermarked image.

D. Extraction Based on k-Means Clustering

If watermarked images are transmitted through an ideal channel, we can directly adopt the inverse operation of (10) to recover host images and watermarks. However, in the real environment, degradation may be imposed on watermarked images due to unintentional attacks, e.g., lossy compression and random noise. Therefore, it is essential to find an effective watermark extraction algorithm so that it can resist unintentional attacks in the lossy environment. Based on the aforementioned embedding model in (10), the MWC histogram of watermarked images are divided into three parts shown in Fig. 3, in which the center part corresponds to watermark bit "0" and others to bit "1." To extract the embedded watermarks, the key issue is to partition these parts dynamically. In the lossy environment, this is very difficult because the histogram distribution of MWC is destroyed by unintentional attacks, as reported in [14]. In this paper, by investigating the effects of unintentional attacks on histogram, we treat the partition as a clustering problem with a certain number of clusters and adopt the k-means clustering algorithm [18], [19] to tackle this problem for simplicity.Similar to the embedding process, we first decompose the watermarked image with 5/3 IWT and construct the MWC histogram by calculating the MWCs of blocks of interest in the sub-band C_0^{HL} . Let $S^w = [\,S_1^w, \ldots, S_m^w\,]$ be the obtained MWCs, F = [$f_1, \ldots, f_\mu$] be the cluster centers, and g =[$g_1, \ldots, g_\mu$] be the set of clusters, wherein μ is the number of clusters. The above classification process is summarized in Table V. Particularly, the initial cluster centers are given by considering the features of the embedding process, e.g.,F = {τ min (Sw) , 0, τ max (Sw)} for μ = 3, to improve the efficiency of classification. Based on the results of classification the embedded watermarks can be extracted by

$$b_k^r = \begin{cases} 0, & \text{if } S_k^w \in \text{Class II} \quad (13) \\ 1, & \text{if } S_k^w \in \text{Class I or Class III} \end{cases}$$

Algorithm-2: Embeddding Procedure of the Proposed Framework

Input: A t-bit host image *I with the size of 2Mx 2N ,a watermark sequence b =[$b_{1,\ldots,}b_m$*]* and block size hxw.
 Output:The watermarked image I^w
1. Apply PIPA to host image *I to ontain the adjusted image I*^{t}, and record the locations of the pixels changed by PIPA:
2. Decompose *I*^{t}using 5/3 IWT and devide
   The sub-band C_0^{HL} into n nonoverlapping blocks with size of h x w;
3. Compute the MWCs of all the blocks with (2) and obtain S = [$S_1, \ldots, S_k, \ldots, Sn$];
4. Retain blocks of interest with the threshold constraint in (3) and construct SQH

5.   Perform EPWM to compute the watermark strength

$$\lambda = \frac{\alpha}{M \ x \ N} \sum_{i=1}^{M} \sum_{j=1}^{N} JND_{\rho}^{w} \ (i,j)$$

6.   For k=1 to m do

7.   Embed the kth watermark with $S_{w}^{k} = S_{k} + \beta\lambda b_{k}$

8.   End for

9.   Recondtruct the watermark image I^{w} with inverse 5/3 IWT

Algorithm-3: Extraction Procedure of the Proposed Framework

Input: A watermarked image I^{W} *with the size of 2Mx 2N , block size h x w , watermark strength* λ *and the*

locations of the *pixel changed by PIPA.*

 Output:The recovered watermarke sequence b^{r} image I^{r} .

1.   Decompose I^{w} using 5/3 IWT and devide
     The sub-band C_{0}^{HL} into n nonoverlapping blocks with size of h x w;

2.   Compute the MWCs of all the blocks of interest with with (2) and obtain $S^{w} = [S_{1}^{w} , \ldots , S_{m}^{w}]$;

3.   For k=1 to m do

4.   Extract the embedded watermarks

$$b_{k}^{r} = \begin{cases} 0, & \text{if } S_{k}^{w} \in \text{Class II} & \text{for } \mu = 3 \quad (13) \\ 1, & \text{if } S_{k}^{w} \in \text{Class I or Class III} \end{cases}$$

5 Recover the MWCs with $S_{k}^{r} = S_{k}^{w} - \beta\lambda b_{k}^{r}$

6 End for

7 Perform inverse IWT follwed by PIPA to obtain the recovered image I^{r}

8 Return the Recovered watermark b^{r} andimage I^{r}

For $\mu = 3$, in which S_{w}^{k} is the kth MWC, brk is the extracted watermark bit, and Classes I–III denote the

obtained set of clusters. Thereafter, we recover the MWCs with $S_{k}^{r} = S_{k}^{w} - \beta\lambda b_{k}^{r}$, which are identical to the

original ones in the lossless environment. After the IWT reconstruction, the inverse operation of (1) is applied to
the pixels changed by PIPA in the embedding process to recover host images. As
mentioned earlier, the side information including the block size, watermark strength, and loations of the pixels
changed by PIPA, should be transmitted to the receiver side, which is important for the recovery of watermarks
and host images, and also leads to nonblindness of the proposed framework to some extent. In summary, the
embedding and extraction processes of the proposed framework are depicted in the discussion.

IV. Simulation Results

In our experiments, the robustness, reversibility, invisibility, capacity, and run-time complexity are used to
evaluate the performance. In particular, the pure capacity is calculated in bits/pixel (b/ps) and the invisibility is
measured by PSNR, defined as

$$PSNR = 10\log\left(\frac{255^{2}}{MSE}\right) \qquad\qquad (14)$$

$$\text{MSE} = \frac{1}{4MN} \sum_{I=1}^{2M} \sum_{J=1}^{2N} \left(I(I,J) - I^{W}(I,J)\right)^{2} \qquad\qquad (15)$$

in which $I \ (i, j \ )$ and $I^{W} \ (i, j \ )$ denote the grayscale values of the pixels at *(i, j)* in the host and watermarked

images.

TABLE I: Simulation values of PSNR, MSE& Ans

Parameter	Value
PSNR	99.89
MSE	0.019
Ans	0.998

Original Image

IWT 5/3 Decomposed image

Watermarked image

extected watermark

Extracted image

Fig 5 a,b,c,d,e: a-Original imamge ,b- IWT 5/3 decomposed image, c- watermarked image, d-extracted watermark, e- Extracted image .
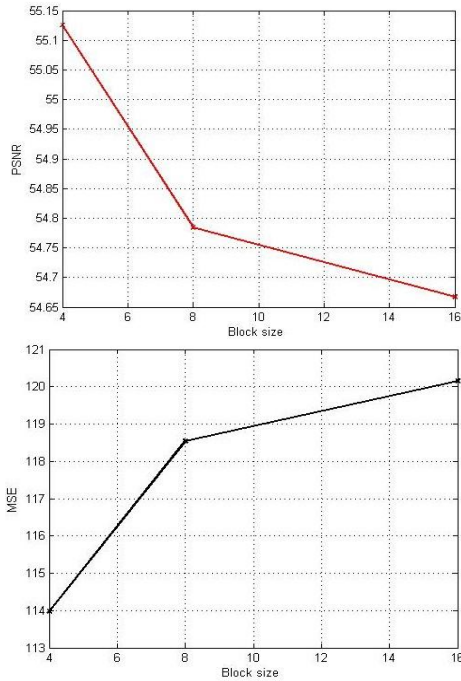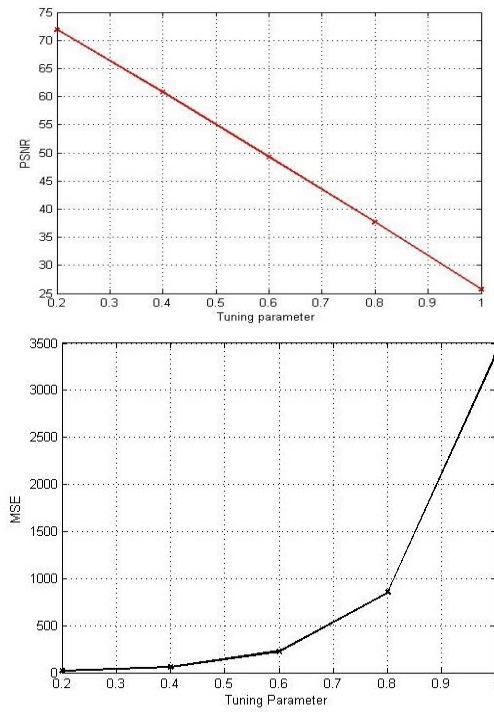
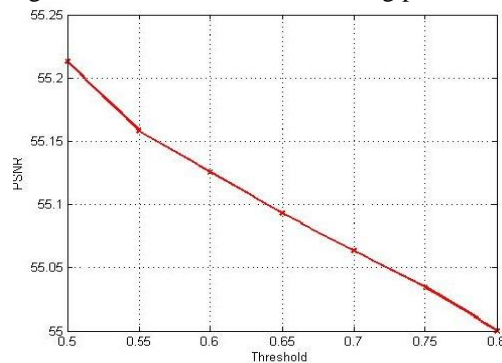Fig 6 a,b: PSNR AND MSE VALUES Vr block size

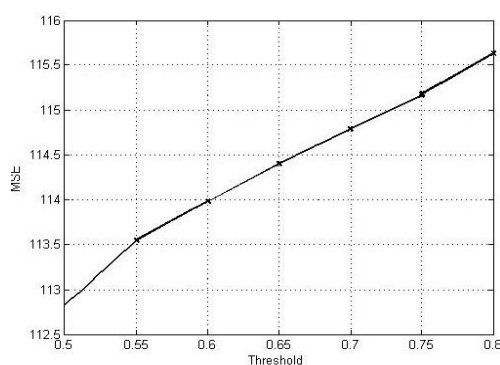Fig 7 a,b: PSNR & MSE Vr Tuning parameter

Fig 8 a,b: MSE and PSNR values Vr Threshold

V. Conclusion

In this paper, we have developed a novel yet pragmatic framework for RRW. It includes carefully designed PIPA,SQH shifting and clustering, and EPWM, each of which handles a specific problem in RRW. PIPA preprocesses host images by adjusting the pixels into a reliable range for satisfactory reversibility. SQH shifting and clustering constructs new watermark embedding and extraction processes for good Robustness and low run-time complexity. EPWM precisely estimates the local sensitivity of HVS and adaptively optimizes the watermark strength for a trade-off between robustness and invisibility. Below are the advantages of this framework: 1) obtains comprehensive performance in terms of reversibility, robustness, invisibility, capacity and run-time complexity; 2) is widely applicable to different kinds of images; and 3) is readily applicable in practice. In future, we will combine the proposed framework with the local feature to further improve robustness. In addition, it is valuable to integrate the merits of sparse representation and probabilistic graphical model into the designing of image watermarking.

REFERENCES

[1] J. Fridrich, M. Goljan, and R. Du, "Lossless data embedding-new paradigm in digital watermarking," *EURASIP J. Appl. Signal Process.*, vol. 2002, no. 1, pp. 185–196, Jan. 2002.

[2] Z. Zhao, N. Yu, and X. Li, "A novel video watermarking scheme in compression domain based on fast motion estimation," in *Proc. Int. Conf. Commun. Technol.*, vol. 2. 2003, pp. 1878–1882.

[3] X. Li, "Watermarking in secure image retrieval," *Pattern Recog. Lett.*, vol. 24, no. 14, pp. 2431–2434, Oct. 2003.

[4] M. Celik, G. Sharma, A. Tekalp, and E. Saber, "Lossless generalized-LSB data embedding," *IEEE Trans. Image Process.*, vol. 14, no. 2, pp. 253–266, Feb. 2005.

[5] J. Tian, "Reversible watermarking using a difference expansion," *IEEE Trans. Circuits Syst. Video Technol.*, vol. 13, no. 8, pp. 890–896, Aug. 2003.

[6] M. Van der Veen, F. Bruekers, A. Van Leest, and S. Cavin, "High capacity reversible watermarking for audio," *Proc. SPIE*, vol. 5020, no.1, pp. 1–11, Jan. 2003.

[7] R. Du and J. Fridrich, "Lossless authentication of MPEG-2 video," in *Proc. IEEE Int. Conf. Image Process.*, vol. 2. Dec. 2002, pp. 893–896.

[8] J. Dittmann and O. Benedens, "Invertible authentication for 3-D-meshes," *Proc. SPIE*, vol. 5020, no. 653, pp. 653–664, Jan. 2003.

[9] L. An, X. Gao, C. Deng, and F. Ji, "Robust lossless data hiding: Analysis and evaluation," in *Proc. Int. Conf. High Perform. Comput. Simul.*, 2010, pp. 512–516.

[10] C. De Vleeschouwer, J. Delaigle, and B. Macq, "Circular interpretation of histogram for reversible watermarking," in *Proc. IEEE Workshop.*

[11] C. De Vleeschouwer, J. Delaigle, and B. Macq, "Circular interpretation of bijective transformations in lossless watermarking for media asset management," *IEEE Trans. Multimedia*, vol. 5, no. 1, pp. 97–105, Mar.2003.

[12] Z. Ni, Y. Shi, N. Ansari, W. Su, Q. Sun, and X. Lin, "Robust lossless image data hiding designed for semi-fragile image authentication," *IEEE Trans. Circuits Syst. Video Technol.*, vol. 18, no. 4, pp. 497–509, Apr. 2008.

[13] D. Zou, Y. Shi, Z. Ni, and W. Su, "A semi-fragile lossless digital watermarking scheme based on integer wavelet transform," *IEEE Trans.Circuits Syst. Video Technol.*, vol. 16, no. 10, pp. 1294–1300, Oct. 2006.

[14] X. Gao, L. An, Y. Yuan, D. Tao, and X. Li, "Lossless data embedding using generalized statistical quantity histogram," *IEEE Trans. Circuits Syst. Video Technol.*, vol. 21, no. 8, pp. 1061–1070, Aug. 2011. *Multimedia Signal Process.*, 2001, pp. 345–350.

[15] C. Chou and Y. Li, "A perceptually tuned subband image coder based on the measure of just-noticeable-distortion profile," *IEEE Trans. Circuits Syst. Video Technol.*, vol. 5, no. 6, pp. 467–476, Dec. 1995.

[16] C. Nafornita, "A new pixel-wise mask for watermarking," in *Proc. ACM Multimedia Secur. Workshop*, 2007, pp. 221–228.

[17] S. Zhang, Q. Tian, G. Hua, Q. Huang, and S. Li, "Descriptive visual words and visual phrases for image applications," in *Proc. ACM Int.Conf. Multimedia*, 2009, pp. 75–84.

[18] T. Xia, D. Tao, T. Mei, and Y. Zhang, "Multiview spectral embedding," *IEEE Trans. Syst., Man, Cybern. B, Cybern.*, vol. 40, no. 6, pp. 1438–1446, Dec. 2010.

[19] T. Zhou and D. Tao, "Fast gradient clustering," in *Proc. NIPS Workshop Discr. Optim. Mach.*